Volume 3
Number 1
7 January 2022
Pages 1–690

Materials Advances

rsc.li/materials-advances

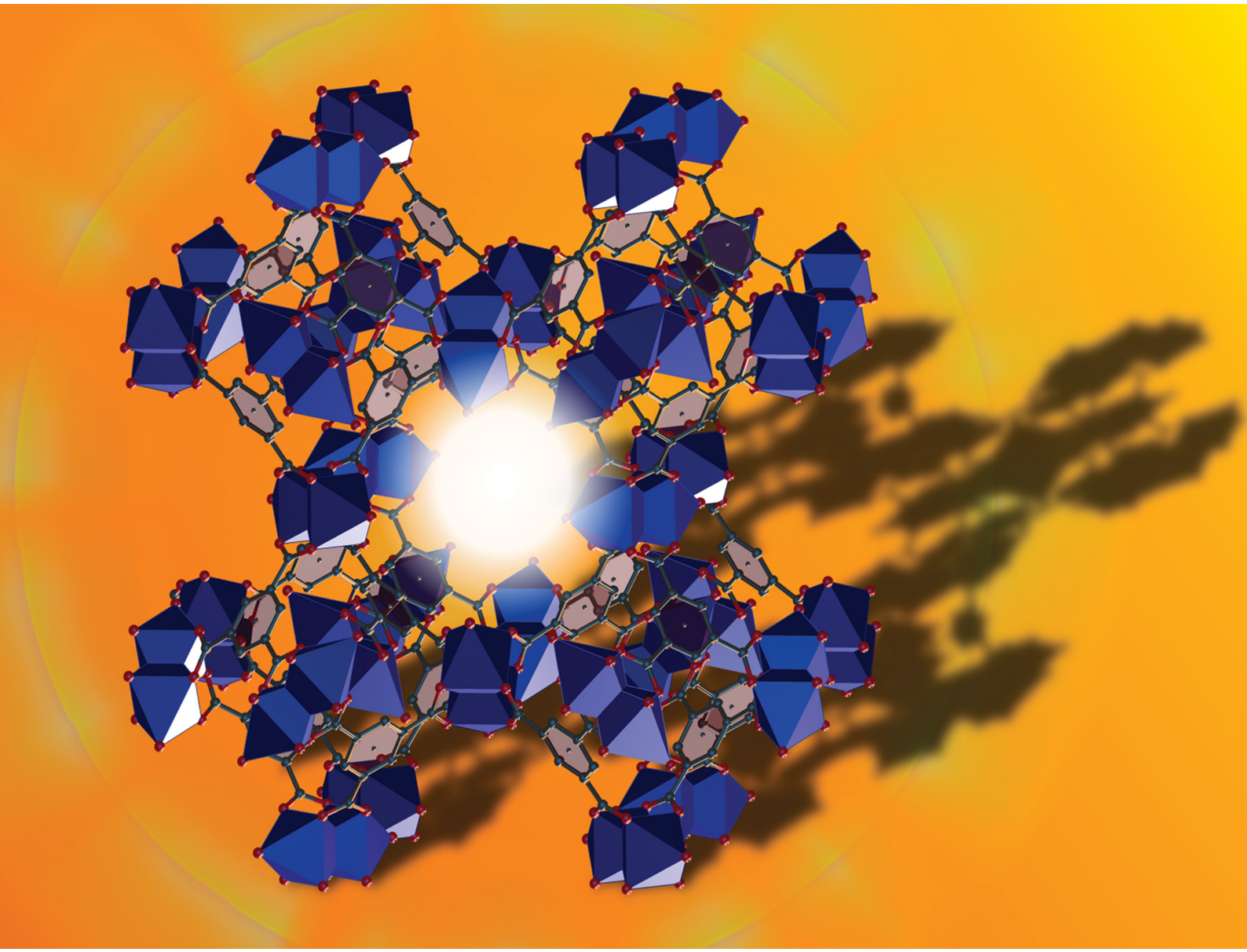

ISSN 2633-5409

ROYAL SOCIETY OF CHEMISTRY

PAPER

Hidetsugu Shiozawa *et al.*

Room temperature synthesis of a luminescent crystalline Cu–BTC coordination polymer and metal–organic framework

Materials Advances

ROYAL SOCIETY OF CHEMISTRY

PAPER

View Article Online
View Journal | View Issue

Cite this: *Mater. Adv.*, 2022, 3, 224

Room temperature synthesis of a luminescent crystalline Cu–BTC coordination polymer and metal–organic framework†

Shiraz Ahmed Siddiqui, [a] Alexander Prado-Roller[b] and Hidetsugu Shiozawa *[ac]

Received 20th September 2021,
Accepted 15th November 2021

DOI: 10.1039/d1ma00866h

rsc.li/materials-advances

Synthesis of crystalline materials is elemental in the field of coordination chemistry towards optical applications. In the present work, coordination between copper and benzene-1,3,5-tricarboxylic acid (BTC) is controlled by adjusting the pH scale of the reaction mixture at room temperature to synthesize two crystalline structures: metal–organic framework HKUST-1 and coordination polymer $Cu(BTC)\cdot 3H_2O$. The post-synthesis transformation of HKUST-1 into $Cu(BTC)\cdot 3H_2O$ is further demonstrated. Single crystals of both structures are studied by multi-laser Raman and luminescence spectroscopy. It is found that both crystals exhibit photoluminescence in the range of 700–900 cm^{-1} within the optical gap of the bulk materials, which can be associated with crystallographic defects. This work gives impetus for the synthesis of large metal–organic crystals based on which optical properties can be studied in depth.

1 Introduction

Organic coordination compounds consist of organic ligands (Lewis base) bound to a central metal ion (Lewis acid).[1–4] The unique and diverse properties of coordination compounds have been proved to be beneficial in the field of electronics, sensors, magnetism and medical research. Coordination polymers are solid-state structures consisting of repeating coordination units to form 1D extended chains, 2D sheets or 3D frameworks.[5–8] Coordination polymers having a porous structure are known as metal–organic frameworks (MOFs).[9–16] Synthesizing large and quality crystals of MOFs benefits in a wide range of applications such as separation, heterogeneous catalysis,[17–19] gas-sorption,[20,21] chromatography,[22,23] optoelectronics, magnetism and sensing applications.[24,25]

Controlling the process of crystallization by pH adjustment is a challenging, yet fascinating process in understanding the chemistry of materials.[26–28] The pH modulating technique was previously utilized to synthesize MOFs.[29–34]

In the present work, the reaction between copper and benzene-1,3,5-tricarboxylic (BTC) acid is controlled by adjusting the pH of the reaction mixture to obtain crystals of two different structures: $Cu_3(BTC)_2(H_2O)_3$ (also known as HKUST-1[35] or MOF-199) and $Cu(BTC)\cdot 3H_2O$ (see Fig. 1).

HKUST-1 is typically synthesized using a hydrothermal/solvothermal method. The high-temperature synthesis yields larger crystals, but the problem is that a significant amount of Cu_2O is obtained as a by-product. This by-product remains in the pores of the framework and reduces the specific surface area thereby causing hinderance in gas absorption.[36] Thus, room-temperature synthesis is beneficial. Our pH-controlled synthesis procedure will help the community to synthesize quality and large crystals of HKUST-1 at room temperature.

In turn, copper(II) based coordination polymers are some of the well studied compounds in the field of natural science and medical research. Owing to the antibacterial activity, low toxicity and potential as biomaterials, these compounds are gaining interest among researchers.[37] In the present work, large crystals of $Cu(BTC)\cdot 3H_2O$ are synthesized at room temperature under weak acid conditions *i.e.* pH greater than 2.1. Single crystal X-ray diffraction (SXRD) reveals that the structure is composed of 1D zig-zag chains interconnected by hydrogen bonding which makes the structure stable and generates a layered coordination network.[38]

The knowledge acquired through the pH-controlled synthesis helps us transform the porous HKUST-1 framework into $Cu(BTC)\cdot 3H_2O$. This process is particularly useful as MOFs sustain the porosity capable of absorbing harmful gases which can be a threat to the environment when the MOFs decompose. Our technique to use water is a fast, efficient and economical method of transforming the framework into non-porous coordination solids for safe disposal.

[a] *Faculty of Physics, University of Vienna, Boltzmanngasse 5, 1090 Vienna, Austria. E-mail: hidetsugu.shiozawa@univie.ac.at, hide.shiozawa@jh-inst.cas.cz*
[b] *Department of Inorganic Chemistry, University of Vienna, Währinger Straße 42, 1090, Vienna, Austria*
[c] *J. Heyrovsky Institute of Physical Chemistry, Czech Academy of Sciences, Dolejskova 3, 182 23 Prague 8, Czech Republic*

† Electronic supplementary information (ESI) available. CCDC 2069999 and 2070000. For ESI and crystallographic data in CIF or other electronic format see DOI: 10.1039/d1ma00866h

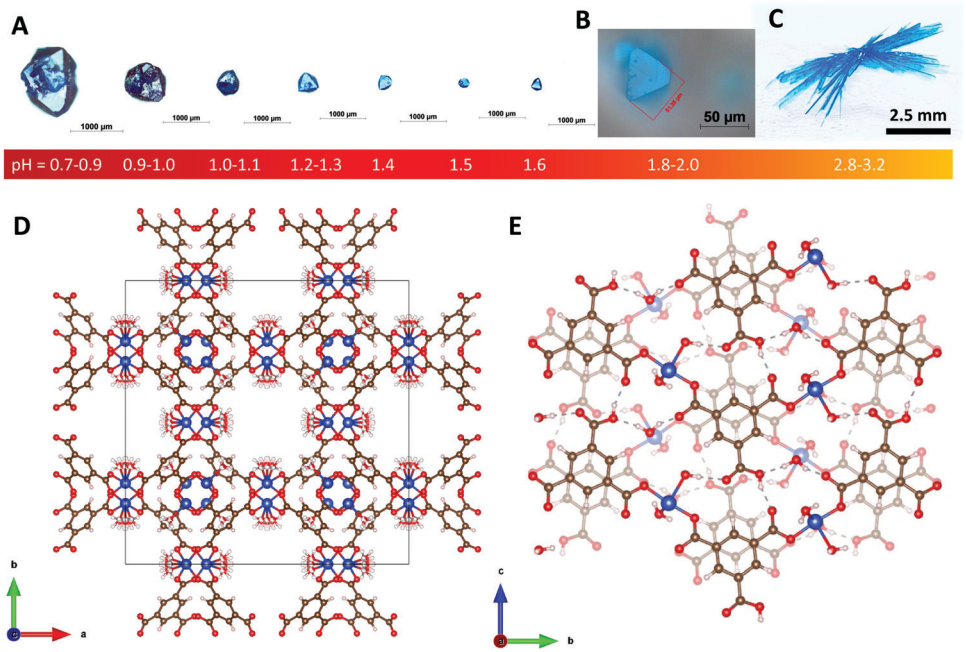

Fig. 1 (A) Seven HKUST-1 crystals synthesized with HNO_3 in the pH range 0.7–1.6. (B) HKUST-1 crystal synthesized without any pH adjustment. (C) Cu(BTC)·$3H_2O$ crystals synthesized in the pH range 2.8–3.2. (D) Crystallographic representation of HKUST-1. (E) Crystallographic representation of the Cu(BTC)·$3H_2O$ coordination polymer viewed along the [100] crystallographic axis.

Finally, luminescent properties of both the HKUST-1 framework and Cu(BTC)·$3H_2O$ are examined on their single crystals with multiple visible lasers. It is found that both crystals luminesce in the range 700–900 cm^{-1} with a red excitation laser, that can be attributed to crystallographic defects.

2 Results and discussions

All synthesis demonstrated in this work is done at room temperature. It is found that crystals of HKUST-1 can be synthesized by adjusting the pH of the reaction mixture in the pH range 0.7–1.6 as shown in Fig. 1A, whereas crystals of Cu(BTC)·$3H_2O$ can be synthesized in the pH range 2.2–3.2 as shown in Fig. 1C and 2B–D.

2.1 Synthesis of HKUST-1

First, we present room temperature synthesis of HKUST-1 (crystal size 50–55 micrometers) without additional pH adjustment. Copper nitrate trihydrate $CuNO_3·3H_2O$ (1 mmol) and BTC (1 mmol) is dissolved in a mixture of three solvents (deionised water 4 ml, DMF 4 ml and ethanol 4 ml) *i.e.* in a volume ratio (V.R.) of 1 : 1 : 1 (pH = 1.8–2.0). After 16–20 hours, crystals of HKUST-1 are formed at the bottom of the vial (pH = 2.1). A clear depiction of the morphology of the as-synthesized HKUST-1 crystal is shown in Fig. 1B. The crystal size is approximately 50 μm across. The homogeneity range is shown in Fig. S1 in the ESI.† An SXRD analysis confirms the well-known structure of HKUST-1 MOF as depicted in Fig. 1D. See the ESI† for more details.

Much larger crystals can be obtained in more acidic conditions prepared by adding 0.1 ml of nitric acid (HNO_3) in the aforementioned 12 ml reaction mixture of V.R. = 1 : 1 : 1. The resulting pH scale is in the range 0.7–0.9. After 8–10 days, crystals of HKUST-1 can get as large as ~1–1.2 mm, as shown in Fig. 1A. More examples of such crystals are shown in Fig. S2 in the ESI.† The size can be controlled by adjusting the pH of

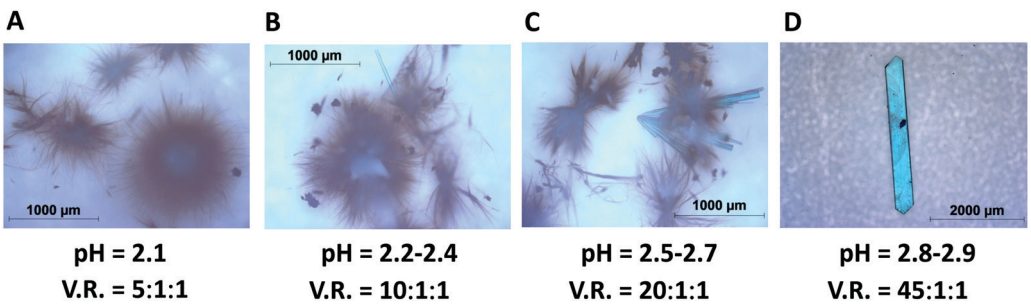

Fig. 2 Crystals and whiskers of Cu(BTC)·$3H_2O$ synthesized at different pH scales. V.R. stands for the volume ratio of three solvents (deionised water, DMF, and ethanol).

the reaction mixture in the range from 0.7 to 2.0, as shown in Fig. 1A. Similarly, large crystals of HKUST-1 in the size range ~0.9–1.0 mm can also be obtained by using 37% hydrochloric acid (HCl) instead of HNO_3 and copper(II) chloride ($CuCl_2$) instead of $CuNO_3{\cdot}3H_2O$. Their crystal size and morphology are shown in Fig. S3 in the ESI.†

It has been reported previously that large crystals of MOFs can be synthesized *via* slow reactions.[22,39] Specifically, large crystals of HKUST-1 could be synthesized in acidic conditions.[23] Deprotonation of BTC is a prerequisite for HKUST-1 growth. In our pH dependent synthesis, HKUST-1 crystals grow larger when a strong acid, HCl or HNO_3, is added in the reaction mixture. The increased amount of H^+ in the mixture inhibits the deprotonation of the BTC ligand. A reduced amount of BTC^{3-} anion leads to slowing down the nucleation and further growth of fewer crystals may be possible.

2.2 Synthesis of Cu(BTC)·3H$_2$O

When the pH is adjusted to exceed 2.1 by adding excess water in the reaction mixture to get a volume ratio of V.R. = 5 : 1 : 1, another type of crystal is formed. Fig. 1C shows this large crystal obtained 2–3 weeks after mixing the precursors. SXRD analysis reveals the structure of Cu(BTC)·3H_2O as shown in Fig. 1E. At pH = 2.1, tiny whiskers appear in 3–4 hours as shown in Fig. 2A. This indicates the point of nucleation. When the pH is increased to 2.2–2.4 (V.R. = 10 : 1 : 1), both tiny whiskers and bar-shaped crystals grow in 12–16 hours as shown in Fig. 2B. A further increase in pH to 2.5–2.7 (V.R. = 20 : 1 : 1) accelerates the crystal growth, resulting in more bar-shaped crystals observed in 16–20 hours as shown in Fig. 2C. At pH = 2.8–2.9 (V.R. = 45 : 1 : 1), the crystal growth is optimized for the formation of only large bar-shaped crystals as shown in the micrograph taken after 18–22 hours in Fig. 2D.

HKUST-1 is not stable in this condition to be demonstrated as the transformation of HKUST-1 to Cu(BTC)·3H_2O in Section 2.4. SXRD evidences that two of the three carboxyl groups of the BTC ligand are coordinated to the Cu^{2+} ion and form zig-zag chains that are linked *via* hydrogen bonding facilitated by the third uncoordinated/protonated carboxyl group and coordinated water molecules (see Fig. 3). The stability of the structure relies on hydrogen bonding of the copper-coordinated water molecules and the pi stacking of the BTC ligands.[38]

2.3 Structure of Cu(BTC)·3H$_2$O

The crystallographic representations of the Cu(BTC)·3H_2O packing structure along the [100], [001] and [010] crystallographic axes are shown in Fig. 3A–C, respectively. For further and detailed information regarding the structure of HKUST-1 and Cu(BTC)·3H_2O, see Section S2 in the ESI.†

The crystal structure is monoclinic with space group $P21/n$ and lattice parameters a = 6.7654, b = 18.8135, c = 8.5144; $\alpha = \gamma = 90°$, $\beta = 92.439°$. The empirical formula of the structure is $C_9H_{10}CuO_9$. This structure was previously reported.[37,38,40–42] Fig. 3A shows the 2D layer of Cu–BTC. Each copper is coordinated to two BTC and three water molecules in the distorted square pyramidal or pentacoordinate geometry.[38,42] BTC consists of three carboxyl groups attached to the benzene ring. Two of the three carboxyl groups of the ligand are coordinated to the metal ion *via* one oxygen to form the zig-zag Cu–BTC polymeric chain. The other oxygen atoms contribute to the hydrogen bonding (dotted line) between the Cu–BTC chains. The Cu–BTC layers are held together by a combination of hydrogen bonding (dotted line) and π–π stacking of the BTC ligand (see Fig. 3B and C). The distance between the adjacent planes is approximately 3.4 Å.

2.4 Transformation of HKUST-1 to Cu(BTC)·3H$_2$O

One of the major concerns in MOF research is that the porous framework can absorb harmful gases. These harmful gases trapped in the pores of the framework can cause threats to the environment. Our results strongly suggest that post-synthesis transformations between HKUST-1 and Cu(BTC)·3H_2O can be possible by adjusting the pH of the reaction mixture. Indeed, when crystals of HKUST-1 are immersed in deionised water to get the pH range 2.8–3.2 suitable for obtaining Cu(BTC)·3H_2O (see Fig. 2D), the HKUST-1 crystals transform into Cu(BTC)·3H_2O in 18–22 hours. The reason behind this conversion is that the water molecule coordinates the metal site of the framework which results in increased coordination around the metal site. As a result, hydrolysis takes place and the organic ligand (BTC) is displaced away from the

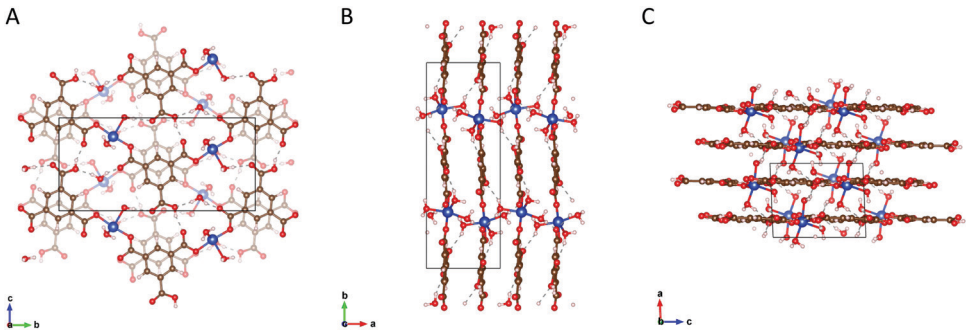

Fig. 3 Panels (A, B and C) shows the structures of the Cu(BTC)·3H_2O coordination polymer along the [100], [001] and [010] crystallographic planes, respectively.

framework. Ultimately, the metal hydroxide remains along with the protonated linker.[42]

2.5 Raman spectroscopy

Fig. 4 shows the Raman spectra of HKUST-1 and Cu(BTC)·3H_2O measured with a green laser (wavelength λ = 514.5 nm) focused on the single crystals in the insets. For HKUST-1, the bands appearing in the low frequency region *i.e.* below 600 cm^{-1} is due to the copper ions in the framework. The doublet at 177.54 cm^{-1} and 197.63 cm^{-1} indicates that the MOF is hydrated and correspondingly Cu–Cu stretching modes appear.[43–45] The band at 275.49 cm^{-1} is indicative of the Cu–O_w stretching vibration, where O_w represents the oxygen of the water molecule adsorbed on Cu^{2+} ions.

The bands in the range 700–1800 cm^{-1} are mostly due to vibrational modes of the BTC ligand. The C=C stretching modes of the benzene ring are found at 1008.9 and 1615.4 cm^{-1} for HKUST-1,[43,44,46–48] and at 1003.5 and 1614.4 cm^{-1} for Cu(BTC)·3H_2O. The peaks at 745.15 and 829.29 cm^{-1} for HKUST-1 can be attributed to the C–H bending modes.[43,44] The corresponding peak for Cu(BTC)·3H_2O is located at 811.13 cm^{-1}. The peaks assigned to the C–O–O symmetric and C–O–O asymmetric stretching modes are centered at 1464.7 and 1552.6 cm^{-1}, respectively, for HKUST-1,[48,49] and at 1459.8 and 1567.9 cm^{-1} for Cu(BTC)·3H_2O.

2.6 Photoluminescence spectroscopy

Luminescence is a key property of MOFs that can lead to their potential applications in optoelectronic devices.[50–52] The luminescence from HKUST-1 and Cu(BTC)·3H_2O single crystals has been examined using seven different excitation lasers. The photoluminescence spectra of HKUST-1 and Cu(BTC)·3H_2O crystals measured at laser wavelengths λ = 458, 488, 514.5, 531, 568, 633 and 647 nm are shown in Fig. 5. All spectra are normalized by the highest Raman peak. The luminescence peak of HKUST-1 appears in the range 675–1000 nm in the spectra measured at λ = 633 and 647 nm (Fig. 5A). Similarly, the spectra of Cu(BTC)·3H_2O recorded at λ = 633 and 647 nm exhibit the luminescence peak in the same range 675–1000 nm (Fig. 5B). In contrast to HKUST-1, the other luminescence peak is observed in the range 458–600 nm at λ = 458 nm, that can be associated with the optical band gap of the Cu(BTC)·3H_2O (see the UV-Vis spectra in Fig. 6). In both cases, the luminescence intensity at λ = 647 nm increases linearly with the laser power, and no saturation has been observed up to a half milliwatts as shown in the insets of Fig. 5 (see the corresponding power-dependent spectra in Fig. S12A and B in the ESI†). The highly consistent luminescence spectra of HKUST-1 and Cu(BTC)·3H_2O at λ = 647 nm suggest similar types of defects present in both crystals.

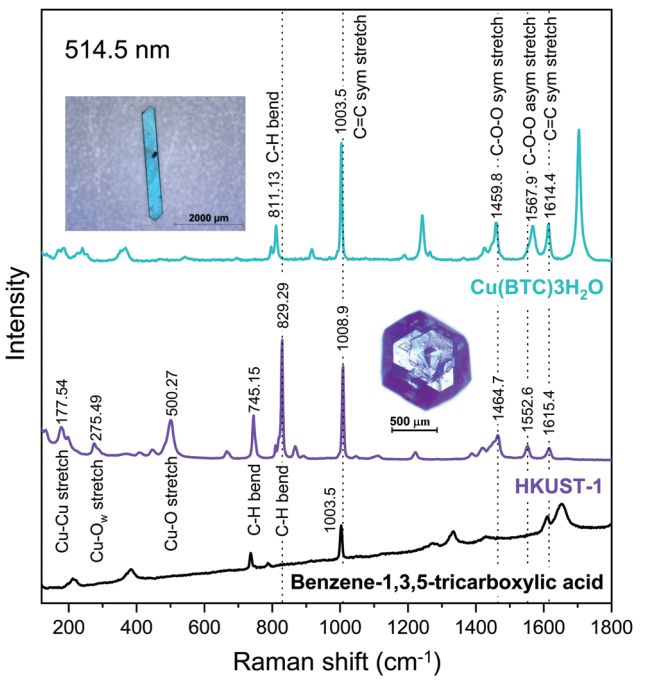

Fig. 4 Raman spectra of HKUST-1 and Cu(BTC)·3H_2O measured at λ = 514.5 nm. The insets show the measured single crystals of HKUST-1 and Cu(BTC)·3H_2O.

Crystallographic defects play vital roles as far as the visible-range optical properties of wide-bandgap MOFs are concerned. Types of defects in HKUST-1 reported thus far include plane dislocations with free COOH groups,[53,54] dislocation growth spirals,[55,56] fractures propagating in the crystal interior,[53] monovalent copper,[54,57,58] metal vacancy,[59] linker vacancy,[60] defective linkers,[61–63] and temporary defects as Brønsted sites.[64] Some defects can be caused post synthesis by exposure to moisture.[42,65] Methods to avoid defects and reconstruct structural defects were reported.[42,66]

Defects can modify the electronic structure of HKUST-1. The reported primary optical band gap of hydrated HKUST-1 is in the range 3–4 eV (approximately 300–400 nm),[57,58,67–70] which can be blue-shifted in defect-engineered HKUST-1[57] or by dehydration.[70]

Fig. 6A shows the UV-Vis spectrum of HKUST-1 crystals. It exhibits the absorption at wavelengths below 450 nm and above 550 nm. The former corresponds to the reported band gap of hydrated HKUST-1, while the latter can be associated with defects. This weak low-frequency visible absorption can be associated with d–d transitions at defective copper pairs leading to the blue colour of defective HKUST-1.[58] This indicates the presence of defects either in the bulk or on the surface of HKUST-1. The luminescence in the wavelength range 675–1000 nm is excited at laser wavelengths of 633 nm (1.96 eV) and 647 nm (1.92 eV) that is in resonance with the optical band gap of defects.[58,70]

Fig. 6B shows the UV-Vis spectrum of Cu(BTC)·3H_2O crystals. The photoluminescence spectra of Cu(BTC)·3H_2O measured at λ = 458, 633 and 647 nm are superposed onto the UV-Vis absorption spectrum. To the best of our knowledge, there have been no reports of UV-Vis absorption and luminescence spectroscopy on Cu(BTC)·3H_2O. The UV-Vis spectrum shows the strong UV absorption at wavelengths below 400 nm and the broad absorption above 600 nm. The long-wavelength tail of the UV absorption coincides with the luminescence

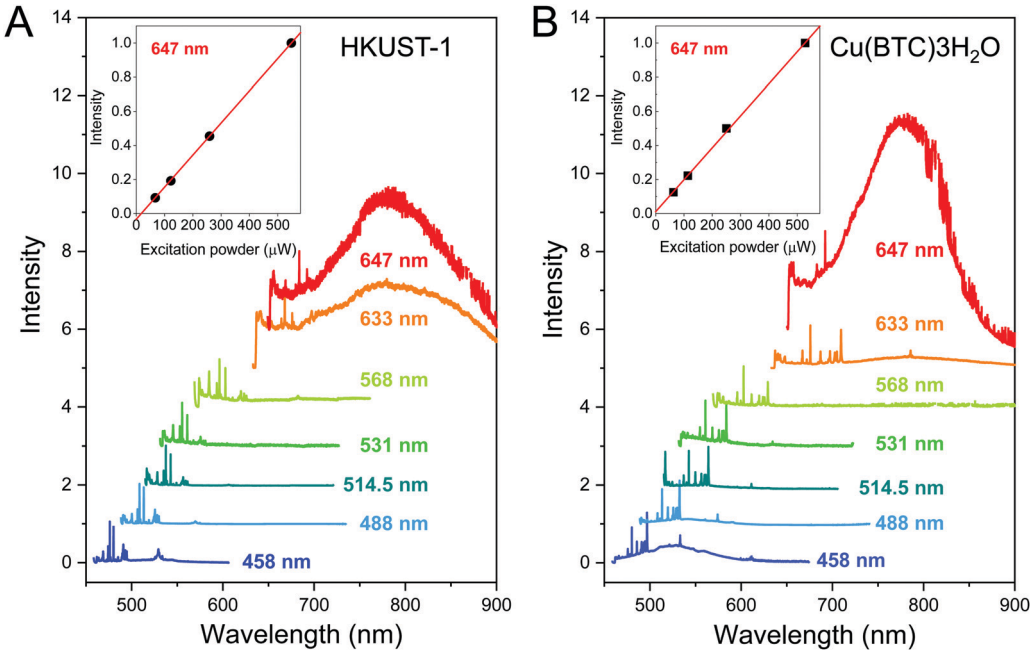

Fig. 5 (A) Photoluminescence spectra (Raman spectra plotted as a function of wavelength) of a HKUST-1 crystal measured on the same spot using seven different lasers λ = 458, 488, 514.5, 531, 568, 633 and 647 nm with laser powers of 0.109, 3.78, 0.617, 0.0712, 1.10, 1.72 and 0.617 mW, respectively. All spectra were normalized by the highest Raman peak. (B) Photoluminescence spectra of a Cu(BTC)·3H_2O crystal measured on the same spot using seven different lasers λ = 458, 488, 514.5, 531, 568, 633 and 647 nm with laser powders of 0.105, 1.37, 0.565, 0.077, 0.708, 1.20, and 0.815 mW, respectively. All spectra were normalized by the highest Raman peak. (insets) The photoluminescence intensity plotted against the laser power at λ = 647 nm.

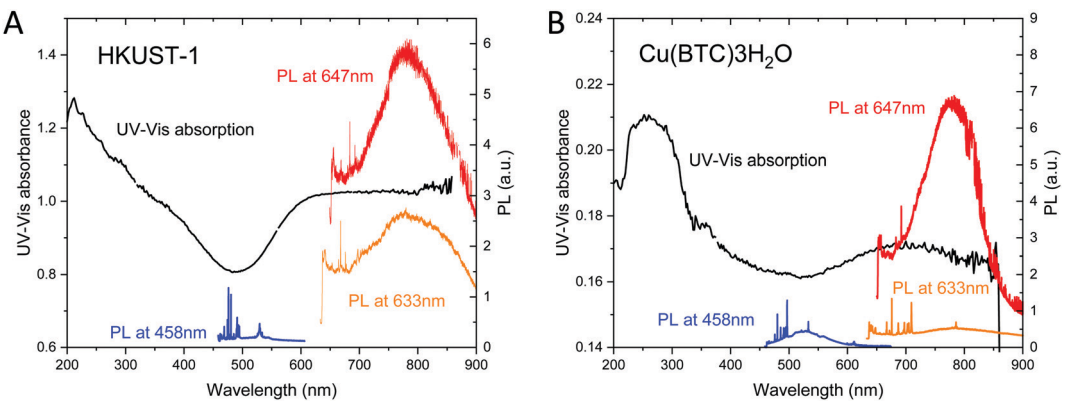

Fig. 6 (A) UV-Vis absorption spectrum of HKUST-1 (black curve). (B) UV-Vis absorption spectrum of Cu(BTC)·3H_2O (black curve). Their photoluminescence (PL) spectra measured at λ = 458, 633, and 647 nm are also plotted in blue, orange and red, respectively.

excited at λ = 458 nm. The broad band above 600 nm leads to the luminescence observed at λ = 647 nm. The much weaker luminescence at 633 nm as compared with HKUST-1 can be attributed to the lower-wavelength absorption onset.

3 Conclusions

The present work has demonstrated that the reaction between copper and benzene-1,3,5-tricarboxylic (BTC) acid can be controlled by adjusting the pH of the precursor solution to obtain millimeter-sized crystals of two different coordination compounds, namely, metal–organic framework HKUST-1 and coordination polymer Cu(BTC)·3H_2O. Crystals of HKUST-1 can be synthesized in the pH range 0.7–0.9, whereas Cu(BTC)·3H_2O in the pH range 2.8–3.2. The post-synthesis transformation from HKUST-1 to Cu(BTC)·3H_2O is possible, which can be useful as means for environmentally-friendly disposal of the MOF. Both species are found to be luminescent. HKUST-1 exhibits luminescence in the range 675–1000 nm that can be associated with crystallographic defects. Cu(BTC)·3H_2O in turn is luminescent in the ranges 458–600 nm and 675–1000 nm, that are in-line

with the UV-Vis absorption spectrum. The present work demonstrates band-gap engineering by the coordination chemistry and defect-induced luminescence in bulky crystals, that in unison will pave the way for optical applications of coordination polymers and MOFs.

Conflicts of interest

There are no conflicts to declare.

Acknowledgements

This work was financially supported by the Austrian Science Fund (FWF), project no. P30431-N36, the Czech Science Foundation (GACR), project no. 19-15217S, the Austrian Federal Ministry of Education, Science and Research (BMBWF) and OeAD-GmbH through Scientific & Technological Cooperation (WTZ) program, project no. CZ 18/2019, and the Ministry of Education, Youth and Sports of the Czech Republic (MEYS) through V4-Japan joint research program, project no. 8F21010. We thank S. Loyer and A. Stangl for technical assistance.

References

1 T. Damhus, R. M. Hartshorn, A. T. Hutton and N. G. Connelly, Nomenclature of inorganic chemistry - iupac recommendations, *Chem. Int.*, 2005, **27**(6), 25–26.
2 M.ichael O'Keeffe, M.axim A. Peskov, S.tuart J. Ramsden and O.mar M. Yaghi, . The Reticular Chemistry Structure Resource (RCSR) Database of, and Symbols for, Crystal Nets, *Acc. Chem. Res.*, 2008, **41**(Suppl. 12), 1782–1789.
3 S. R. Batten, N. R. Champness, X.-M. Chen, J. Garcia-Martinez, S. Kitagawa, L. Ohrstrom, M. O'Keeffe, M. Paik Suh and J. Reedijk, . Coordination polymers, metal-organic frameworks and the need for terminology guidelines, *CrystEngComm*, 2012, **14**(9), 3001–3004.
4 R. R. Crichton, Basic coordination chemistry for biologists, in *Biological Inorganic Chemistry*, ed. R. R. Crichton, Elsevier, Oxford, 2nd edn, 2012, ch. 2, pp. 21–34.
5 S. R. Batten, S. M. Neville and D. R. Turner, *Coordination polymers: Design, analysis and application*, Royal Soc Chemistry, Thomas Graham House, Science park, Cambridge, CB4 4WF, CAMBS, England, 2009, pp. 1–424.
6 S. R. Batten, N. R. Champness, X.-M. Chen, J. Garcia-Martinez, S.usumu Kitagawa, L. Ohrstrom, M. O'Keeffe, M. Paik Suh and J. Reedijk, Terminology of metal–organic frameworks and coordination polymers (IUPAC Recommendations 2013), *Pure Appl. Chem.*, 2013, **85**(8), 1715–1724.
7 L. Ohrstrom, Let's Talk about MOFs-Topology and Terminology of Metal-Organic Frameworks and Why We Need Them, *Crystals*, 2015, **5**(1), 154–162.
8 E. R. Engel and J. L. Scott, Advances in the green chemistry of coordination polymer materials, *Green Chem.*, 2020, **22**(12), 3693–3715.
9 J. L. C. Rowsell and O. M. Yaghi, Metal-organic frameworks: a new class of porous materials, *Microporous Mesoporous Mater.*, 2004, **73**(1-2), 3–14.
10 J. R. Long and O. M. Yaghi, The pervasive chemistry of metal-organic frameworks, *Chem. Soc. Rev.*, 2009, **38**(5), 1213–1214.
11 K. Biradha, A. Ramana and J. J. Vittal, Coordination Polymers Versus Metal–Organic Frameworks, *Cryst. Growth Des.*, 2009, **9**(7), 2969–2970.
12 H. Li, M. Eddaoudi, M. O'Keeffe and O. M. Yaghi, Design and synthesis of an exceptionally stable and highly porous metal–organic framework, *Nature*, 1999, **402**(6759), 276–279.
13 A. K. Cheetham and C. N. R. Rao, There's room in the middle, *Science*, 2007, **318**(5847), 58–59.
14 C. Janiak and J. K. Vieth, MOFs, MILs and more: concepts, properties and applications for porous coordination networks (PCNs), *New J. Chem.*, 2010, **34**(11), 2366–2388.
15 Z.-G. Gu, D.-J. Li, C. Zheng, Y. Kang, C. Woell and J. Zhang, MOF-Templated Synthesis of Ultrasmall Photoluminescent Carbon-Nanodot Arrays for Optical Applications, *Angew. Chem., Int. Ed.*, 2017, **56**(24), 6853–6858.
16 Z.-G. Gu and J. Zhang, Epitaxial growth and applications of oriented metal-organic framework thin films, *Coord. Chem. Rev.*, 2019, **378**(SI), 513–532.
17 A. Dhakshinamoorthy, M. Alvaro and H. Garcia, Commercial metal-organic frameworks as heterogeneous catalysts, *Chem. Commun.*, 2012, **48**(92), 11275–11288.
18 A. Corma, H. Garcia and F. X. L. I. Llabres i Xamena, Engineering Metal Organic Frameworks for Heterogeneous Catalysis, *Chem. Rev.*, 2010, **110**(8), 4606–4655.
19 Y. Wen, J. Zhang, Q. Xu, X.-T. Wu and Q.-L. Zhu, Pore surface engineering of metal-organic frameworks for heterogeneous catalysis, *Coord. Chem. Rev.*, 2018, **376**, 248–276.
20 R. Babarao, J. Jiang and S. I. Sandler, Molecular Simulations for Adsorptive Separation of CO_2/CH_4 Mixture in Metal-Exposed, Catenated, and Charged Metal–Organic Frameworks, *Langmuir*, 2009, **25**(9), 5239–5247.
21 O. Zybaylo, O. Shekhah, H. Wang, M. Tafipolsky, R. Schmid, D. Johannsmann and C. Woell, A novel method to measure diffusion coefficients in porous metal-organic frameworks, *Phys. Chem. Chem. Phys.*, 2010, **12**(28), 8092–8097.
22 S. Han, Y. Wei, C. Valente, I. Lagzi, J. J. Gassensmith, A. Coskun, J. F. Stoddart and B. A. Grzybowski, Chromatography in a Single Metal-Organic Framework (MOF) Crystal, *J. Am. Chem. Soc.*, 2010, **132**(46), 16358–16361.
23 L. Li, F. Sun, J. Jia, T. Borjigin and G. Zhu, Growth of large single MOF crystals and effective separation of organic dyes, *CrystEngComm*, 2013, **15**(20), 4094–4098.
24 J. W. Brown, B. L. Henderson, M. D. Kiesz, A. C. Whalley, W. Morris, S. Grunder, H. Deng, H. Furukawa, J. I. Zink, J. F. Stoddart and O. M. Yaghi., Photophysical pore control in an azobenzene-containing metal-organic framework, *Chem. Sci.*, 2013, **4**(7), 2858–2864.
25 J. A. Mason, M. Veenstra and J. R. Long, Evaluating metal-organic frameworks for natural gas storage, *Chem. Sci.*, 2014, **5**(1), 32–51.

26 N. D. Burrows, C. R. H. Hale and R. Lee Penn, Effect of pH on the Kinetics of Crystal Growth by Oriented Aggregation, *Cryst. Growth Des.*, 2013, **13**(8), 3396–3403.

27 N. Fomina, C. A. Johnson, A. Maruniak, S. Bahrampour, C. Lang, R. W. Davis, S. Kavusi and H. Ahmad, An electrochemical platform for localized pH control on demand, *Lab Chip*, 2016, **16**(12), 2236–2244.

28 R.-Q. Chen, Q.-D. Cheng, J.-J. Chen, D.-S. Sun, L.-B. Ao, D.-W. Li, Q.-Q. Lu and D.-C. Yin, An investigation of the effects of varying pH on protein crystallization screening, *CrystEngComm*, 2017, **19**(5), 860–867.

29 C. Gabriel, M. Perikli, C. P. Raptopoulou, A. Terzis, V. Psycharis, C. Mateescu, T. Jakusch, T. Kiss, M. Bertmer and A. Salifoglou, pH-Specific Hydrothermal Assembly of Binary and Ternary Pb(II)-(O,N-Carboxylic Acid) Metal Organic Framework Compounds: Correlation of Aqueous Solution Speciation with Variable Dimensionality Solid-State Lattice Architecture and Spectroscopic Signatures, *Inorg. Chem.*, 2012, **51**(17), 9282–9296.

30 I. Chi-Duran, J. Enriquez, C. Manquian, K. Wrighton-Araneda, W. Canon-Mancisidor, D. Venegas-Yazigi, F. Herrera and D. P. Singh, pH-Controlled Assembly of 3D and 2D Zinc-Based Metal-Organic Frameworks with Tetrazole Ligands, *ACS Omega*, 2018, **3**(1), 801–807.

31 R. Abazari, A. R. Mahjoub, A. M. Z. Slawin and C. L. Carpenter-Warren, Morphology- and size-controlled synthesis of a metal–organic framework under ultrasound irradiation: An efficient carrier for pH responsive release of anti-cancer drugs and their applicability for adsorption of amoxicillin from aqueous solution, *Ultrason. Sonochem.*, 2018, **42**, 594–608.

32 Y. Lv, S. Wang, R. Zhang, D. Zhang, H. Yu and G. Lu, PH-modulated formation of uniform MOF-5 sheets, *Inorg. Chem. Commun.*, 2018, **97**, 30–33.

33 R. Seetharaj, P. V. Vandana, P. Arya and S. Mathew, Dependence of solvents, pH, molar ratio and temperature in tuning metal organic framework architecture, *Arabian J. Chem.*, 2019, **12**(3), 295–315.

34 X. Luo, Q. Zhou, S. Du, J. Li, L. Zhang, K. Lin, H. Li, B. Chen, T. Wu, D. Chen, M. Chang and Y. Liu, One-Dimensional Porous Hybrid Structure of Mo2C-CoP Encapsulated in N-Doped Carbon Derived from MOF: An Efficient Electrocatalyst for Hydrogen Evolution Reaction over the Entire pH Range, *ACS Appl. Mater. Interfaces*, 2018, **10**(49), 42335–42347.

35 S. S. Y. Chui, S. M. F. Lo, J. P. H. Charmant, A. G. Orpen and I. D. Williams, A chemically functionalizable nanoporous material [Cu-3(TMA)(2)(H_2O)(3)](*n*), *Science*, 1999, **283**(5405), 1148–1150.

36 K.-S. Lin, A. K. Adhikari, C.-N. Ku, C.-L. Chiang and H. Kuo, Synthesis and characterization of porous HKUST-1 metal organic frameworks for hydrogen storage, *Int. J. Hydrogen Energy*, 2012, **37**(18), 13865–13871.

37 A. Rauf, J. Ye, S. Zhang, Y. Qi, G. Wang, Y. Che and G. Ning, Copper(II)-based coordination polymer nanofibers as a highly effective antibacterial material with a synergistic mechanism, *Dalton Trans.*, 2019, **48**, 17810–17817.

38 A. Kojtari, P. J. Carroll and H.-F. Ji, Metal organic framework (MOF) micro/nanopillars, *CrystEngComm*, 2014, **16**(14), 2885–2888.

39 J. M. Garcia-Garfido, J. Enríquez, I. Chi-Durán, I. Jara, L. Vivas, F. J. Hernández, F. Herrera and D. P. Singh, Millimeter-scale zn(3-ptz)2 metal-organic framework single crystals: Self-assembly mechanism and growth kinetics, *ACS Omega*, 2021, **6**(27), 17289–17298.

40 R. Pech and J. Pickardt, Catena-Triaqua-Mu-[1,3,5-benzenetricarboxylato(2-)]-Copper(II), *Acta Crystallogr., Sect. C: Cryst. Struct. Commun.*, 1988, **44**(6), 992–994.

41 G. W. Peterson, G. W. Wagner, A. Balboa, J. Mahle, T. Sewell and C. J. Karwacki, Ammonia Vapor Removal by Cu-3(BTC)(2) and Its Characterization by MAS NMR, *J. Phys. Chem. C*, 2009, **113**(31), 13906–13917.

42 G. Majano, O. Martin, M. Hammes, S. Smeets, C. Baerlocher and J. Perez-Ramirez, Solvent-Mediated Reconstruction of the Metal-Organic Framework HKUST-1 (Cu-3(BTC)(2)), *Adv. Funct. Mater.*, 2014, **24**(25), 3855–3865.

43 C. Prestipino, L. Regli, J. G. Vitillo, F. Bonino, A. Damin, C. Lamberti, A. Zecchina, P. L. Solari, K. O. Kongshaug and S. Bordiga, Local structure of framework Cu(II) in HKUST-1 metallorganic framework: Spectroscopic characterization upon activation and interaction with adsorbates, *Chem. Mater.*, 2006, **18**(5), 1337–1346.

44 N. R. Dhumal, M. P. Singh, J. A. Anderson, J. Kiefer and H. J. Kim, Molecular Interactions of a Cu-Based Metal-Organic Framework with a Confined Imidazolium-Based Ionic Liquid: A Combined Density Functional Theory and Experimental Vibrational Spectroscopy Study, *J. Phys. Chem. C*, 2016, **120**(6), 3295–3304.

45 S. D. Worrall, M. A. Bissett, P. I. Hill, A. P. Rooney, S. J. Haigh, M. P. Attfield and R. A. W. Dryfe, Metal-organic framework templated electrodeposition of functional gold nanostructures, *Electrochim. Acta*, 2016, **222**, 361–369.

46 J. Cortes-Suarez, V. Celis-Arias, H. Beltran, I. A. Tejeda-Cruz, I. A. Ibarra, J. E. Romero-Ibarra, E. Sanchez-Gonzalez and S. Loera-Serna., Synthesis and Characterization of an SWCNT@HKUST-1 Composite: Enhancing the CO_2 Adsorption Properties of HKUST-1, *ACS Omega*, 2019, **4**(3), 5275–5282.

47 N. Marshall, W. James, J. Fulmer, S. Crittenden, A. B. Thompson, P. A. Ward and G. T. Rowe, Polythiophene Doping of the Cu-Based Metal-Organic Framework (MOF) HKUST-1 Using Innate MOF-Initiated Oxidative Polymerization, *Inorg. Chem.*, 2019, **58**(9), 5561–5575.

48 F. S. Gentile, M. Pannico, M. Causa, G. Mensitieri, G. D. Palma, G. Scherillo and P. Musto, Metal defects in HKUST-1 MOF revealed by vibrational spectroscopy: a combined quantum mechanical and experimental study, *J. Mater. Chem.*, 2020, **8**(21), 10796–10812.

49 C. Petit, B. Mendoza, D. O'Donnell and T. J. Bandosz, Effect of Graphite Features on the Properties of Metal-Organic Framework/Graphite Hybrid Materials Prepared Using an in Situ Process, *Langmuir*, 2011, **27**(16), 10234–10242.

50 M. D. Allendorf, C. A. Bauer, R. K. Bhakta and R. J. T. Houk, Luminescent metal-organic frameworks, *Chem. Soc. Rev.*, 2009, **38**(5), 1330–1352.
51 Y. Cui, Y. Yue, G. Qian and B. Chen, Luminescent Functional Metal-Organic Frameworks, *Chem. Rev.*, 2012, **112**(Supp. 2), 1126–1162.
52 J. Heine and K. Mueller-Buschbaum, Engineering metal-based luminescence in coordination polymers and metal–organic frameworks, *Chem. Soc. Rev.*, 2013, **42**(24), 9232–9242.
53 R. Ameloot, F. Vermoortele, J. Hofkens, F. C. De Schryver, D. E. De Vos and M. B. J. Roeffaers, Three-Dimensional Visualization of Defects Formed during the Synthesis of Metal-Organic Frameworks: A Fluorescence Microscopy Study, *Angew. Chem., Int. Ed.*, 2013, **52**(1), 401–405.
54 Z. Fang, B. Bueken, D. E. D. Vos and R. A. Fischer, Defect-Engineered Metal-Organic Frameworks, *Angew. Chem., Int. Ed.*, 2015, **54**(25), 7234–7254.
55 M. Shoaee, M. W. Anderson and M. P. Attfield, Crystal Growth of the Nanoporous Metal-Organic Framework HKUST-1 Revealed by In Situ Atomic Force Microscopy, *Angew. Chem., Int. Ed.*, 2008, **47**(44), 8525–8528.
56 M. Shoeaee, J. R. Agger, M. W. Anderson and M. P. Attfield, Crystal form, defects and growth of the metal organic framework HKUST-1 revealed by atomic force microscopy, *CrystEngComm*, 2008, **10**(6), 646–648.
57 Z. Fang, J. P. Duerholt, M. Kauer, W. Zhang, C. Lochenie, B. Jee, B. Albada, N. Metzler-Nolte, A. Poeppl, B. Weber, M. Muhler, Y. Wang, R. Schmid and R. A. Fischer, Structural Complexity in Metal-Organic Frameworks: Simultaneous Modification of Open Metal Sites and Hierarchical Porosity by Systematic Doping with Defective Linkers, *J. Am. Chem. Soc.*, 2014, **136**(27), 9627–9636.
58 K. Müller, K. Fink, L. Schöttner, M. Koenig, L. Heinke and C. Wöll, Defects as color centers: The apparent color of metal-organic frameworks containing Cu2+ -based paddle-wheel units, *ACS Appl. Mater. Interfaces*, 2017, **9**(42), 37463–37467, PMID: 28976730.
59 W. Zhang, M. Kauer, P. Guo, S. Kunze, S. Cwik, M. Muhler, Y. Wang, K. Epp, G. Kieslich and R. A. Fischer, Impact of synthesis parameters on the formation of defects in hkust-1, *Eur. J. Inorg. Chem.*, 2017, **2017**(5), 925–931.
60 S. Bordiga, L. Regli, F. Bonino, E. Groppo, C. Lamberti, B. Xiao, P. S. Wheatley, R. E. Morris and A. Zecchina, Adsorption properties of hkust-1 toward hydrogen and other small molecules monitored by ir, *Phys. Chem. Chem. Phys.*, 2007, **9**(21), 2676–2685.
61 T. Steenhaut, N. Gregoire, G. Barozzino-Consiglio, Y. Filinchuk and S. Hermans, Mechanochemical defect engineering of HKUST-1 and impact of the resulting defects on carbon dioxide sorption and catalytic cyclopropanation, *RSC Adv.*, 2002, **10**(34), 19822–19831.
62 L. Guo, J. Du, C. Li, G. He and Y. Xiao, Facile synthesis of hierarchical micro-mesoporous hkust-1 by a mixed-linker defect strategy for enhanced adsorptive removal of benzothiophene from fuel, *Fuel*, 2021, **300**, 120955.
63 D. F. Sanchez, J. Ihli, D. Zhang, T. Rohrbach, P. Zimmermann, J. Lee, C. N. Borca, N. Böhlen, D. Grolimund and J. A. van Bokhoven, *et al.*, Spatio-chemical heterogeneity of defect-engineered metal-organic framework crystals revealed by full-field tomographic X-ray absorption spectroscopy, *Angew. Chem.*, 2021, **133**(18), 10120–10127.
64 M. Polozij, M. Rubes, J. Cejka and P. Nachtigall, Catalysis by Dynamically Formed Defects in a Metal-Organic Framework Structure: Knoevenagel Reaction Catalyzed by Copper Benzene-1,3,5-tricarboxylate, *ChemCatChem*, 2014, **6**(10), 2821–2824.
65 M. Todaro, G. Buscarino, L. Sciortino, A. Alessi, F. Messina, M. Taddei, M. Ranocchiari, M. Cannas and F. M. Gelardi, Decomposition process of carboxylate mof hkust-1 unveiled at the atomic scale level, *J. Phys. Chem. C*, 2016, **120**(23), 12879–12889.
66 K. Müller, N. Vankova, L. Schöttner, T. Heine and L. Heinke, Dissolving uptake-hindering surface defects in metal-organic frameworks, *Chem. Sci.*, 2019, **10**, 153–160.
67 F. A. Sofi, K. Majid and O. Mehraj, The visible light driven copper based metal-organic-framework heterojunction:h-kust-1@ag-ag3po4 for plasmon enhanced visible light photocatalysis, *J. Alloys Compd.*, 2018, **737**, 798–808.
68 C. Fan, H. Dong, Y. Liang, J. Yang, G. Tang, W. Zhang and Y. Cao, Sustainable synthesis of hkust-1 and its composite by biocompatible ionic liquid for enhancing visible-light photocatalytic performance, *J. Cleaner Prod.*, 2019, **208**, 353–362.
69 Y. Qiao, Q. Han, D. Li, H. Li, B. Wei, G. Che, W. Jiang and W. Guan, Construction of novel Ag/HKUST-1/g-C3N4 towards enhanced photocatalytic activity for the degradation of pollutants under visible light, *RSC Adv.*, 2019, **9**(71), 41591–41602.
70 N. K. Kulachenkov, D. Sun, Y. A. Mezenov, A. N. Yankin, S. Rzhevskiy, V. Dyachuk, A. Nominé, G. Medjahdi, E. A. Pidko and V. A. Milichko, Photochromic free mof-based near-infrared optical switch, *Angew. Chem., Int. Ed.*, 2020, **59**(36), 15522–15526.